

Friction and wear behavior of three-dimensional braided carbon fiber/epoxy composites under lubricated sliding conditions

Y. Z. WAN*, H. L. LUO, Y. L. WANG, Y. HUANG, Q. Y. LI, F. G. ZHOU
School of Materials Science and Engineering, Tianjin University, Tianjin, 300072, People's Republic of China
E-mail: yzwan@tju.edu.cn, yzwantju@yahoo.com

G. C. CHEN
Aerospace Research Institute of Materials and Processing Technology, Beijing, 100076, People's Republic of China

The friction and wear characteristics of three-dimensional (3D) braided carbon fiber-epoxy (C_{3D}/EP) composites under lubricated sliding conditions against a quenched medium-carbon steel counterface were studied. Wear tests were performed under different loads at two velocities. Comparative wear tests under dry conditions were carried out to investigate the influence of lubrication. Tribological properties of the C_{3D}/EP composites with various fiber loadings and two different fiber-matrix adhesion strengths were assessed. It was found that the lubricated contact promoted lower wear rates and friction coefficients. Compared to dry sliding, the tribological performance of the C_{3D}/EP composites under lubrication was less dependent on fiber content, fiber-matrix bonding, load, and velocity than dry sliding. The worn surfaces of the C_{3D}/EP composites were analyzed by scanning electron microscopy (SEM) to explore the relevant mechanisms.

© 2005 Springer Science + Business Media, Inc.

1. Introduction

Composite materials are among the most rapidly growing classes of materials and are finding more and more medical applications such as orthopedic implants, internal fixation devices and external fixators, etc. [1–3]. Three-dimensional (3D) composites are superior to unidirectional fiber composites in impact damage and delamination tolerances, ease of handling during fabrication, and fracture toughness. This has made them an important class of composite materials for structural and tribological applications. When used as orthopedic implants, the 3D composites are subjected to not only mechanical stresses and attacks from media within human body, but also tribological loading conditions, which may cause friction and eventually unpredictable failures of the composite parts. It was reported that excessive friction can cause the prosthesis to work loose within the bone, resulting in pain and instability [4]. Carbon fiber debris was found to cause an adverse reaction in the adjacent tissue [5] and result in adverse cellular reactions [6] which led to bone resorption loosening and the need for a revision operation [7, 8].

Relative systematic studies have been carried out to generate data for conventional mechanical properties of 3D composites, but not for tribological properties.

With respect to tribological performance, vast literature is available on the exploitation of short and long fibers and solid lubricants for improving the wear performance of engineering polymers. Researchers have already shown how the friction and wear of fiber-polymer composites depend on fiber type and geometry and its orientation, type of matrix, fiber loading, counterpart material, sliding conditions, etc. [9–11]. Surprisingly, little is reported on the wear performance of fabric reinforced composites. The existing literature focuses on investigations of wear behavior of woven fabric reinforced composites [12, 13]. To date, no data are available regarding the tribological performance of the 3D braided fiber composites.

Our previous work suggests that 3D braided carbon fiber/epoxy resin (C_{3D}/EP) composites are potential materials for orthopedic usage [14]. It is necessary to assess their tribological properties, particularly inside the human body condition (wet conditions). To this end, a phosphate buffer solution (PBS) was selected as the lubrication in this study.

The main objective of this study was, therefore, to investigate the friction and wear characteristics of the C_{3D}/EP composites in PBS lubrication. Emphasis was placed on comparing the responses of the 3D

*Author to whom all correspondence should be addressed.

TABLE I Characteristics of fiber and matrix used in the present study

Materials	Fabric	Matrix
Type	Four-directional	E-51
Tensile strength (MPa)	2800	60
Tensile modulus (GPa)	200	3.2
Elongation at break (%)	1.5	1.8
Density (kg m ⁻³)	1760	1200
Braiding angle (Degree)	20	—
Filament number (k)	6	—

composites under different sliding conditions. For this purpose, wear tests of the 3D composites with varying material parameters (fiber loading and fiber-matrix bonding) were performed at various testing conditions (load and velocity).

2. Experimental

2.1. Materials

The raw materials were polyacrylonitrile (PAN)-based carbon fibers supplied by Shanghai Xinxing Carbon Co., Ltd. (Shanghai, China). They possess the following characteristics: tensile strength, 2000 MPa; tensile modulus, 196 GPa; diameter, 6–8 μm; density, 1.75 g cm⁻³. The preforms, 3D four-directional fabrics, prepared by Tianjin Polytechnic University, Tianjin, China, were described earlier [15]. According to the manufacturer, the 3D braided preform was constructed by the intertwining or orthogonal interlacing of two sets of yarns-braiders and axials to form a fully integrated structure. The preform was spanned by four groups of parallel yarns which formed two sets of parallel planes and intersected orthogonally. A home-made epoxy resin (bis-phenol A type) was used as the matrix material. The details of the fiber and the matrix are listed in Table I.

2.2. Fiber surface treatment

It is well accepted that suitable surface treatment of carbon fibers helps enhance the interfacial bonding between the fibers and the matrix. In our previous studies [16], oxidation in air was adopted, which was proven to considerably enhance the fiber-matrix bonding and therefore improve the mechanical properties of the C_{3D}/EP composites. In the present study, 3D braided fabrics were surface treated in air at 450°C for an hour after desizing by immersing in an organic solvent for 24 h, which is the optimal surface treatment condition [16].

2.3. Preparation of samples

The C_{3D}/EP composite specimens were produced by a vacuum assisted resin transfer molding (VARTM) process. Five braided fabrics with a nominal size of 160 × 12 × 2 mm were placed in a mould. A toughened epoxy resin and a curing agent were intimately mixed at ambient temperature and degassed at 70°C for 30 min in a vacuum oven. The mould containing the braided fabrics was also equilibrated at 70°C prior to resin pouring.

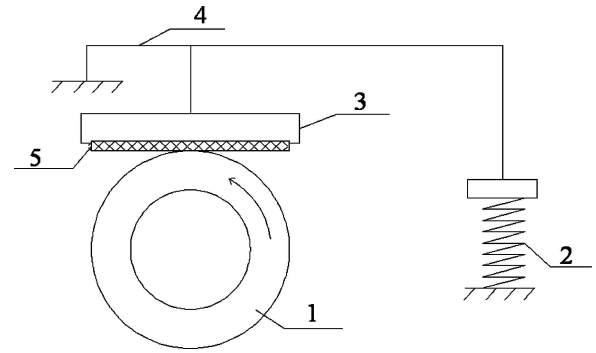


Figure 1 Schematic diagram of the wear tester 1—steel ring, 2—spring, 3—specimen holder, 4—lever, 5—specimen.

The degassed mixed resin was then introduced into the mould under a pressure of 0.4–0.6 MPa and assisted by the vacuum. The introduction of resin continued until no bubbles were observed within the resin flowing out from the exit of the mould. The evacuating process did not stop until the completion of resin introduction. The mould was then put into an oven for curing (at 90°C for 2 h) and postcuring (at 140°C for 3 h).

2.4. Sliding wear tests

Specimens were immersed in PBS for five weeks prior to wet wear tests. Comparative dry wear tests were also performed in an attempt to evaluate the influence of sliding conditions. The specimens for dry sliding wear tests were not immersed in PBS. The sliding wear was carried out on an MM200 tester as shown in Fig. 1. The coupons were inserted in a metal base during wear tests. The counterface used was a quenched medium carbon steel ring with a hardness of HRC 52 and a R_a of 0.40 μm. The normal force applied to the specimens was controlled by adjusting the spring (see Fig. 1). Wear tests were performed at normal loads of 50, 150, and 250 Newtons and sliding velocities of 0.42 and 0.84 m/s. In all the wear tests, the braiding direction of the 3D composites was kept parallel to the sliding direction. The specimens were removed and cleaned after a predetermined duration to measure the width of the wear scratches with a three-dimensional profilometer. The specific wear rate, calculated by dividing the wear volume by the product of load and sliding distance, was employed in this work. The volume loss, ΔV of the specimens were calculated by

$$\Delta V = B \left[\frac{\pi R^2}{180} \arcsin \frac{b}{2R} - \frac{b\sqrt{R^2 - \frac{b^2}{4}}}{2} \right] \quad (1)$$

The coefficient of friction, μ and the specific wear rate, W_s determined as specific volume loss were calculated from

$$\mu = \frac{T}{RN} \quad (2)$$

$$W_s = \frac{\Delta V}{NS} \quad (3)$$

In the above three equations, R is the radius of the counterpart in mm, b and B are the width (in mm) of the wear scratches and width of the testing coupons, respectively. μ is the coefficient of friction. T stands for the frictional torque (Nm) and N the normal load (N) applied to the wear specimens. W_s represents the specific wear rate in mm^3/Nm , ΔV the volume loss (mm^3), and S the total sliding distance (m).

At least three coupons cut in dimensions of $30 \times 7 \times 2$ mm were tested for each group so as to minimize data scattering. The average values and standard deviations from the three replicate tests are reported.

2.5. SEM observations

Microscopic examination of the worn surfaces of the specimens subjected to different conditions was carried out by means of an XL30 model environmental scanning electron microscope (ESEM). The worn surfaces of the specimens were gold coated prior to observation. Some wear debris was collected and inspected by SEM.

3. Results and discussion

3.1. Friction and wear behaviors under different stages

Experimental results of the friction coefficient and the specific wear rate are plotted against sliding distance in Figs 2 and 3, respectively, for a fixed load of 150 N and a fixed velocity of 0.42 m/s. The corresponding curves under dry conditions are also given in the two figures. Clearly, the friction coefficient and the specific wear rate of the 3D epoxy composites decreased with operating duration at early stages under lubricated conditions. Afterwards, the friction coefficient and the specific wear rate remained unchanged. The C_{3D}/EP composites showed a similar pattern under dry sliding. The plausible explanation for the decreasing trend at early stages is: in the early stages, the so-called running-in period, the surfaces of both the composites and the steel counterparts were rough and thus strong 'interlocking' took place, resulting in high friction coefficients. As the wear process continued, the rough profiles of the

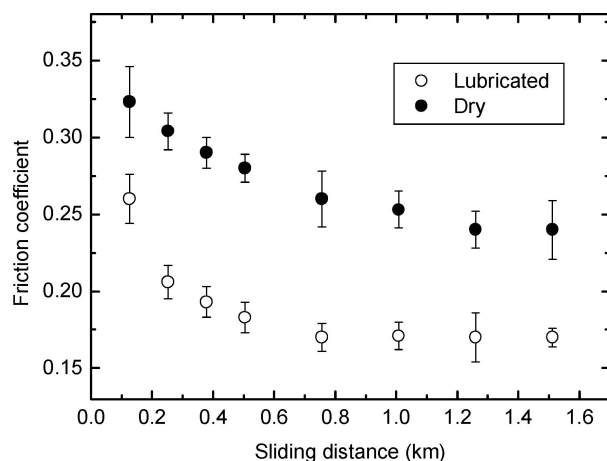


Figure 2 Variation of friction coefficient of the C_{3D}/EP composites with sliding distance under PBS lubrication ($V_f = 0.38$, 150 N/0.42 m/s).

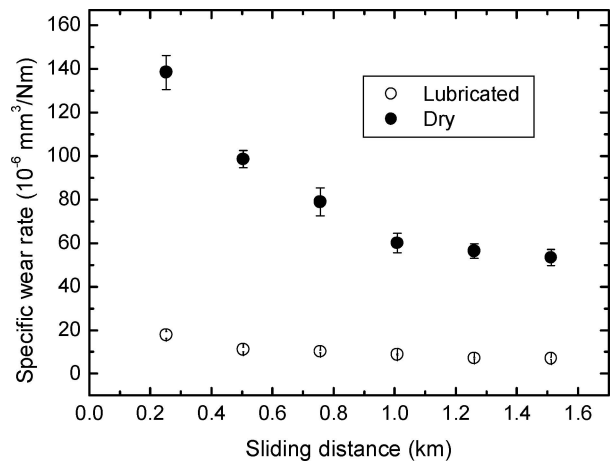


Figure 3 Variation of specific wear rate of the C_{3D}/EP composites with sliding distance under PBS lubrication ($V_f = 0.38$, 150 N/0.42 m/s).

steel counterparts and the composites were gradually smoothed. Consequently, the friction coefficient and wear rate became lower.

It is worthwhile to mention that the friction coefficients and the specific wear rates at dry sliding were higher than at lubricated conditions, suggesting the role of lubrication in reducing wear. It is known that contrary results have been reported on the effect of liquid medium (such as deionized water, sea water and other aqueous solutions) on the wear and friction of polymer matrix composites [17]. Lancaster [18] reported an increase in wear and friction in water for the carbon/epoxy composites while a reduction for glass/epoxy was also reported [19]. Explanations are also different. On the one hand, the changes of wear and friction with the presence of water are believed to be related to modification of structure surface layer of polymers and/or modification of counterface by water [20]. On the other hand, water lubrication is believed to remove the debris from the rubbing region so as to reduce wear and friction [21]. We believe that either mechanism may dominate, depending on the structure and property of matrix materials, nature of fibers and fiber/matrix interfaces. In the present work, the lower coefficients of friction and the much lower specific wear rates under lubrication than dry contact can be interpreted as follows: Firstly, presence of a lubricating film was observed between the mating surfaces, which plays a critical role in decreasing coefficient friction and wear. Secondly, under lubricated conditions, the cooling effect of the PBS prevents temperature rise on counterface surfaces, which, in turn, reduces the possibility of the occurrence of local microwelding at the tips of the major asperities of the surfaces, thus reducing the wear loss and the friction coefficient. Finally, the cleansing effect of the PBS also prevents the debris from aggregating between the two counterface surfaces. In this way, the presence of hard particles between or embedded in one or both of the two surfaces in relative motion is diminished, which, in turn, lessens the development of abrasive wear, hence reducing the specific wear rate and the coefficient of friction.

Typical worn surfaces of the C_{3D}/EP composites under dry and lubricated conditions are presented

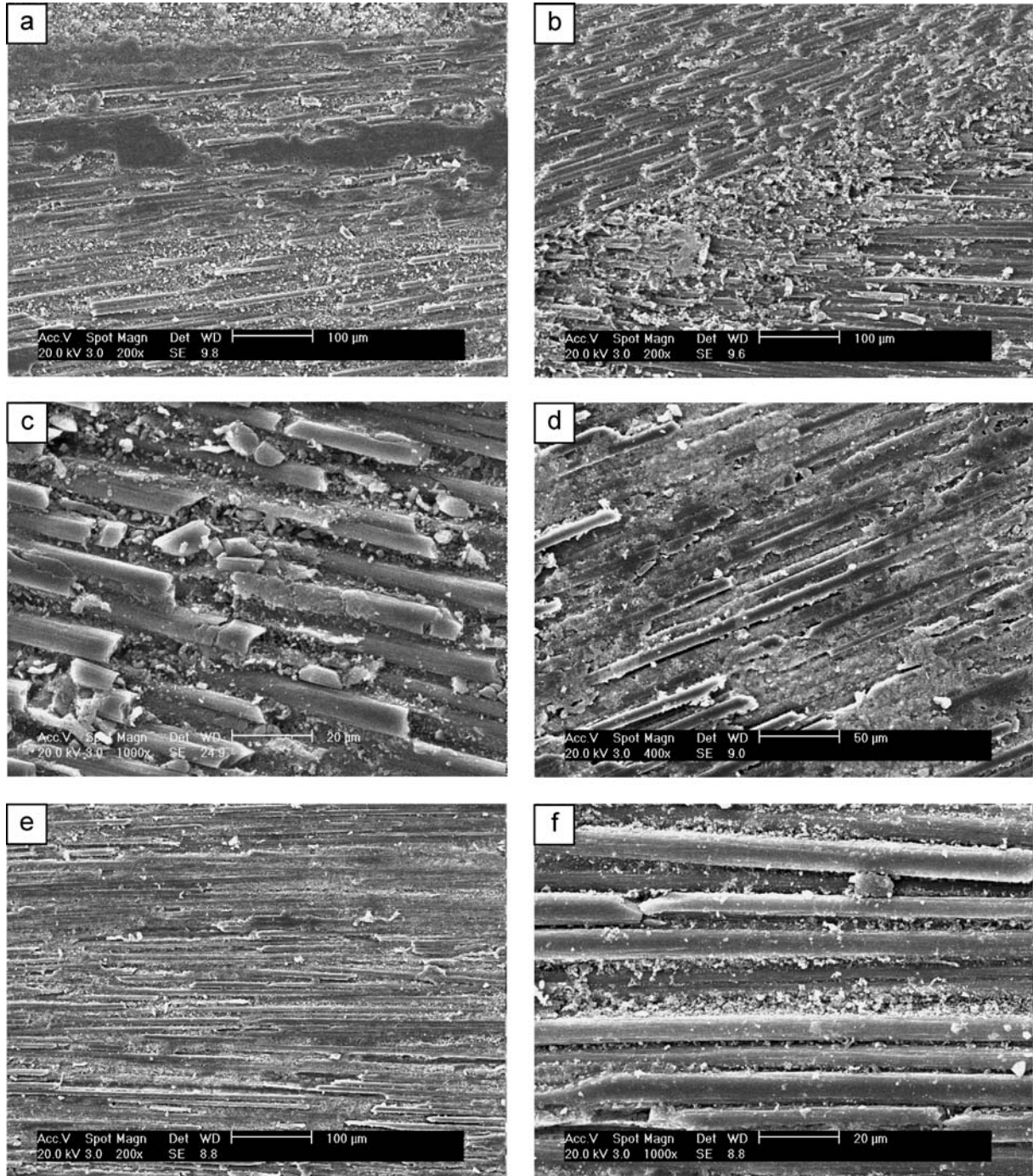


Figure 4 Worn surfaces of the C_{3D}/EP composites under dry (a to c) and lubricated (d to f) conditions (a and d—at 10 min; b, c, e, and f—at 40 min).

in Fig. 4. Fig. 4a shows the worn surface of the C_{3D}/EP composites subjected to 10 min dry sliding (150 N/0.42 m/s). Clearly, the adhesive and abrasive wear mechanisms can be identified. After 40 min dry sliding, the abrasive mechanism dominated (see Figs 4b and c). Comparisons of the worn surfaces shown in Figs 4d–f and Fig. 4a–c reveal significantly different surface features. The worn surfaces under lubricated conditions were clean due to the cleaning action of the lubricant, which supports the cleansing effect mechanism. Only powdery particles adhered to the fibers were observed at a high magnification (see Fig. 4f). Moreover, less fiber breakage (Fig. 4c vs. Fig. 4f) was observed and less matrix peeling-off (Fig. 4a vs. Fig. 4d and Fig. 4b vs. Fig. 4e) was identified under lubrication

than in dry contact at identical sliding distances. This is likely caused mainly by the presence of the lubricating film between the two counterparts which serves to reduce the thrust during wear, hence reducing both fiber breakage and matrix detachment.

3.2. Effect of fiber volume fraction

Fig. 5 details the friction coefficient as a function of fiber volume fraction (V_f). Evidently, the friction coefficient of the C_{3D}/EP composites increased slightly with V_f under dry conditions, while under lubrication the friction coefficient was independent on V_f under the current testing conditions, keeping a constant value of 0.17 ± 0.01 . On the contrary, drastic changes in

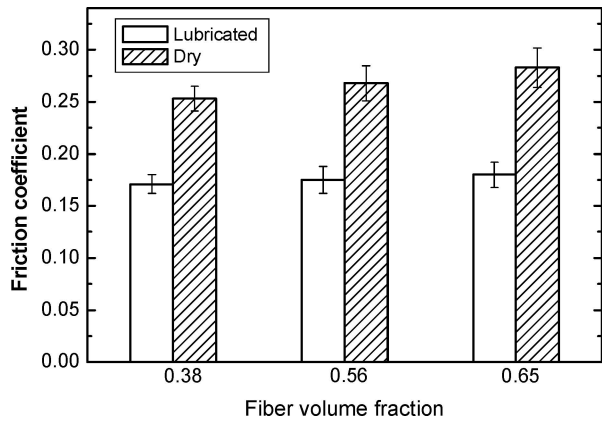


Figure 5 Variation of friction coefficient of the C_{3D}/EP composites with fiber content under PBS lubrication (150 N/0.42 m/s).

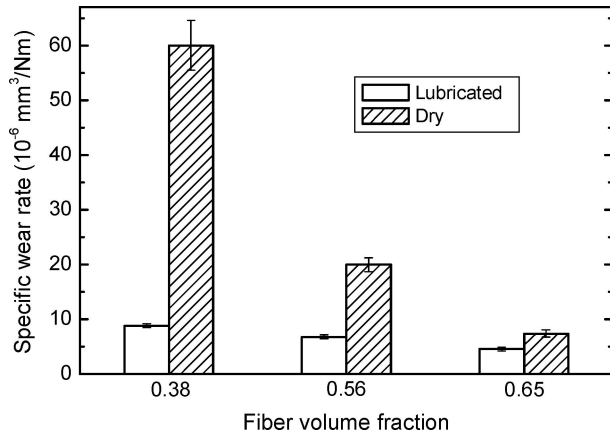


Figure 6 Variation of specific wear rate of the C_{3D}/EP composites with fiber content under PBS lubrication (150 N/0.42 m/s).

the specific wear rate were observed when V_f varied in the range of 0.38 to 0.65 as depicted in Fig. 6. When V_f increased from 0.38 to 0.65, the average specific wear rate of the C_{3D}/EP composites decreased by 88 and 48% under dry and lubricated conditions, respectively. This result suggests that the specific wear rate is more V_f dependent under dry sliding conditions than wet conditions.

3.3. Effect of load and velocity

The effects of load and velocity on the friction coefficient of the C_{3D}/EP composites with a V_f of 0.38 are depicted in Fig. 7. Under dry sliding, the friction coefficient decreased with an increase in either load or velocity. In the case of lubricated sliding, the effects of load and velocity on the friction coefficient were insignificant.

The specific wear rate of the C_{3D}/EP composites ($V_f = 0.38$) is plotted against load in Fig. 8. At least three features can be found from this figure. (1) A significant difference in the specific wear rate existed between lubricated and dry conditions under each load and each velocity condition. The C_{3D}/EP composites demonstrated much lower specific wear rates under lubricated conditions than dry conditions in all cases studied. (2) Compared to the friction coefficient, the specific wear rate was more dependent on load—considerable reduc-

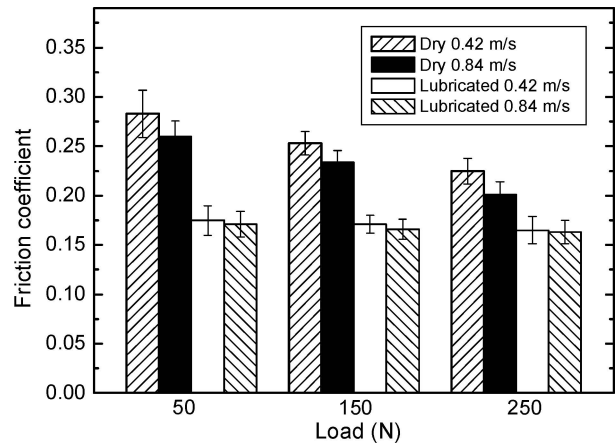


Figure 7 Effects of load and velocity on friction coefficient of the C_{3D}/EP composites ($V_f = 0.38$).

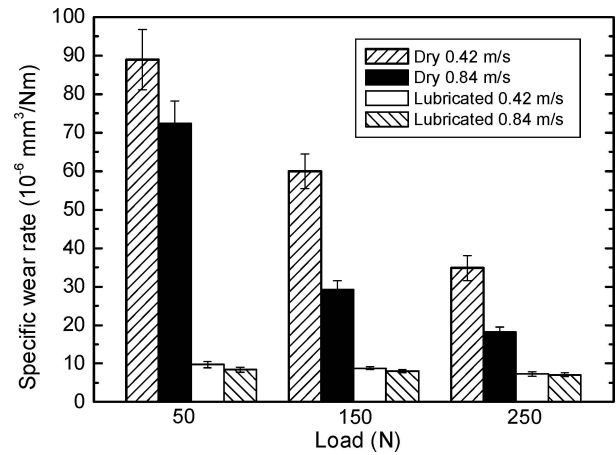


Figure 8 Effects of load and velocity on specific wear rate of the C_{3D}/EP composites ($V_f = 0.38$).

tions in the specific wear rate were observed when the load increased from 50 N to 150 N, and then to 250 N. The average specific wear rate decreased by 60.9, 75.0, 24.7, and 15.8% under dry sliding and a velocity of 0.42 m/s, dry and 0.84 m/s, lubricated and 0.42 m/s, and lubricated and 0.84 m/s, respectively, when the load increased from 50 to 250 N. The corresponding values for the friction coefficient were 20.5, 22.7, 5.7, and 4.7%. The highest and lowest specific wear rates were observed at 50 N and 250 N, respectively, for both dry and lubricated conditions at both velocities (0.42 and 0.84 m/s). (3) The effect of velocity on the specific wear rate was significant under dry conditions while the specific wear rate showed no significant changes under lubrication in all cases. The data presented in Figs 7 and 8 indicated that the specific wear rate and the friction coefficient were less sensitive to the changes of load and velocity under lubrication than dry contact. This is likely to be attributed to the presence of the lubricating film under wet conditions. A similar result was reported by Fisher and co-workers who found that sliding velocity had little effect on friction and wear of ultrahigh molecular weight polyethylene (UHMWPE) when a protein-containing solution, bovine serum, was used as lubricating medium [22].

3.4. Effect of fiber surface treatment

The friction and wear behavior of polymer composites generally depends upon interfacial adhesion. For instance, Zhang *et al.* declared that the improvement in the tribological behavior of PEEK composites with plasma surface treatment came from the improvement in the interface strength of carbon-fiber-reinforced PEEK composites [23]. As reported previously [16], the C_{3D}/EP composites containing treated carbon fibers possessed higher interfacial adhesion, flexural properties and hardness than those containing untreated fibers. In order to assess the dependence of tribological properties on fiber-matrix bonding, two different C_{3D}/EP composites reinforced with, respectively, treated and untreated carbon fibers were prepared, tested under identical testing conditions (150 N/0.42 m/s). They were compared in terms of the changes of the friction coefficient and the specific wear rate with sliding distance. The experimental results are presented in Figs 9 and 10.

One can see from Fig. 9 that the friction coefficients of the C_{3D}/EP composites reinforced with treated carbon fibers were not significantly different from those of the composites with untreated fibers up to a slid-

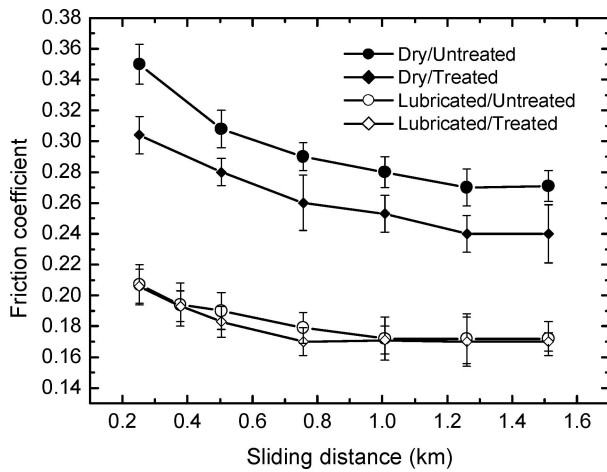


Figure 9 Variation of friction coefficient with sliding distance for the C_{3D}/EP composites reinforced with treated and untreated fibers under dry and lubricated conditions ($V_f = 0.38$, 150 N/0.42 m/s).

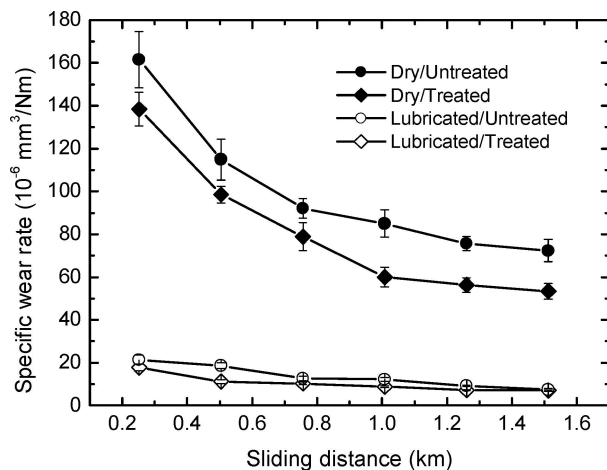


Figure 10 Variation of specific wear rate with sliding distance for the C_{3D}/EP composites reinforced with treated and untreated fibers under dry and lubricated conditions ($V_f = 0.38$, 150 N/0.42 m/s).

ing distance of 1.5 km under lubricated conditions. In contrast, the friction coefficients of the composites reinforced with treated fibers were lower than those of the composites with untreated fibers under dry sliding, indicating the friction coefficient is less sensitive to interfacial adhesion under lubrication than under dry sliding.

Fig. 10 reveals that the 3D composites reinforced with treated carbon fibers showed lower specific wear rates than the composites with untreated fibers under dry sliding. This suggests that higher interfacial adhesion yields better wear resistance. Under lubrication, however, interfacial adhesion exerted little influence on the specific wear rate. Generally speaking, the composites with higher fiber-matrix bonding have better wear resistance as wear loss is inversely proportional to strength and hardness for both adhesive and abrasive wear mechanisms. Furthermore, as proposed by Friedrich *et al.* [24] and Zhang *et al.* [25], high fiber-matrix bonding helps reduce fiber debonding and helps keep the broken fibers in the composite surface, thus preventing the early formation of third-body abrasive. This can elucidate the reduced specific wear rates of the treated composites under dry sliding. The independence of the specific wear rate and the friction coefficient on fiber-matrix bonding under lubrication can be interpreted by the fact that PBS acts as a lubricant and washes away debris between two counterfaces. Therefore, no heavy frictional thrust was applied to the fibers and the matrix and no fiber debonding could happen.

4. Conclusions

The C_{3D}/EP composites exhibited markedly lower friction coefficients and specific wear rates when lubricated. The better tribological properties under PBS lubrication were ascribed to the formation of a lubricating film on the counterfaces, cooling effect and cleansing effect of the PBS. It was found that under dry sliding, the friction coefficient and the specific wear rate decreased with increasing either load or velocity. Furthermore, the specific wear rate was more load and velocity dependent than the friction coefficient under dry contact. Lubrication made the specific wear rate less sensitive to changes in velocity and load. Moreover, the friction coefficient showed little variation with load or velocity under lubrication. Increasing the interfacial bonding strength reduced the friction coefficient and the specific wear rate under drying sliding conditions. Nevertheless, neither friction coefficient nor specific wear rate showed any dependence on fiber-matrix adhesion under lubrication. It is concluded that the friction and wear under lubricated conditions are less sensitive to material parameters (V_f and fiber-matrix bonding) and testing conditions (load and velocity) than under dry sliding.

Acknowledgments

The authors gratefully acknowledge the Tianjin Municipal Natural Science Foundation (Grant No. 013604211), Key Project Program (Grant No.

0113111711), and Municipal Science and Technology Development Program (Grant No. 043111511).

References

1. J. S. BRADLEY, G. W. HASTINGS and C. JOHNSON-NURSE, *Biomaterials* **1** (1980) 38.
2. C. MIGLIARESI, F. NICOLI, S. ROSSI and A. PEGORETTI, *Compos. Sci. Technol.* **64** (2004) 873.
3. J. KETTUNEN, E. A. MA KELA, H. MIETTINEN, T. NEVALAINEN, M. HEIKKILA, T. POHJONEN, P. TORMALA and P. ROKKANEN, *Biomaterials* **19** (1998) 1219.
4. J. PAULO DAVIM, N. MARQUES and A. M. BAPTISTA, *Wear* **251** (2001) 1100.
5. R. S. J. KENNETH and K. T. TSAO, in *Encyclopedic Handbook of Biomaterials and Bioengineering*, Part A: Materials, Vol. 2, edited by D. L. Wise et al. (Marcel Dekker, New York, 1995), p. 1817.
6. D. W. MURRAY and N. RUSHTON, *J. Bone Joint Surgery* **72B** (1990) 988.
7. D. W. HOWIE, B. VERNON-ROBERTS, R. OAKESHOTT and B. MATHEY, *ibid.* **70A** (1988) 257.
8. D. W. LENNOX, B. H. SCHOFIELD, D. F. MCDONALD and L. H. RILEY, *Orthopaedics Relat. Res.* **225** (1987) 171.
9. K. FRIEDRICH, Z. LU and A. M. HAGER, *Theoretical Applied Fracture Mechanics* **19** (1993) 1.
10. C. P. TURSSI, B. M. PURQUERIO and M. C. SERRA, *J. Biomed. Mater. Res. Part B: Appl. Biomater.* **65B** (2003) 280.
11. B. VISHWAMATH, A. P. VERMA and C. V. S. KAMESWARA RAE, *Wear* **145** (1991) 315.
12. J. BIJWE, J. INDUMATHI and A. K. GHOSH, *ibid.* **253** (2002) 803.
13. B. VISHWANATH, A. P. VERMA and C. V. S. RAO, *ibid.* **167** (1993) 93.
14. Y. Z. WAN, Y. L. WANG, G. X. CHENG and K. Y. HAN, *J. Appl. Polym. Sci.* **85** (2002) 1031.
15. Y. Z. WAN, Y. L. WANG, H. L. LUO and J. G. QI, *ibid.* **80** (2001) 367.
16. Y. Z. WAN, Y. L. WANG, F. G. ZHOU, G. X. CHENG and K. Y. HAN, *ibid.* **85** (2002) 1040.
17. O. JACOBS, R. JASKULKA, F. YANG and W. WU, *Wear* **256** (2004) 9.
18. J. K. LANCASTER, *ibid.* **20** (1972) 315.
19. N. S. EL-TAYEB and R. M. GADELRAH, *ibid.* **192** (1996) 112.
20. Y. YAMAMOTO and M. HASHIMOTO, *ibid.* **253** (2002) 820.
21. *Idem*, *ibid.* **257** (2004) 181.
22. J. FISHER, D. DOWSON, H. HAMDZAH and H. L. LEE, *ibid.* **175** (1994) 219.
23. R. ZHANG, A. M. HAEGER, K. FRIEDRICH, Q. SONG and Q. DONG, *ibid.* **181-183** (1995) 613.
24. K. FRIEDRICH, Z. LIU and A. M. HAGER, *ibid.* **190** (1995) 139.
25. H. ZHANG and Z. ZHANG, *Compos. Sci. Technol.* **64** (2004) 2031.

Received 20 December 2004
and accepted 28 March 2005